

12-21-2020

## Natural Convection Air Cooling of Electronic Components in Partially Top Vented Enclosures.

Mohamed Saafan

*Mechanical Power Engineering, Faculty of Engineering, Mansoura University, Egypt,*  
mgmoussa@mans.edu.eg

Follow this and additional works at: <https://mej.researchcommons.org/home>

---

### Recommended Citation

Saafan, Mohamed (2020) "Natural Convection Air Cooling of Electronic Components in Partially Top Vented Enclosures.," *Mansoura Engineering Journal*: Vol. 30 : Iss. 2 , Article 4.  
Available at: <https://doi.org/10.21608/bfemu.2020.131387>

This Original Study is brought to you for free and open access by Mansoura Engineering Journal. It has been accepted for inclusion in Mansoura Engineering Journal by an authorized editor of Mansoura Engineering Journal. For more information, please contact [mej@mans.edu.eg](mailto:mej@mans.edu.eg).

## Natural Convection Air cooling of Electronic Components in Partially top vented Enclosures

التبريد بالحمل الطبيعي لعناصر الكترونية متواجدة في حيز مهوى جزئياً من أعلى

M. G. Mousa

Mechanical Power Engineering Dept., Faculty of Engineering, Mansoura University, Mansoura., Egypt.  
Mgmousa@mans.edu.eg

خلاصة البحث:

في هذا البحث تم عمل دراسة نظرية لانتقال الحرارة بالحمل الطبيعي في حيز مفتوح جزئياً من أعلى بطرق مختلفة. تم وصف الحمل الطبيعي بواسطة كل من معادلة السريان ومعادلات الحركة ومعادلة الطاقة وذلك باستخدام الاحداثيات الكرتيزية. الحيز الذي تمت عليه الدراسة يشابه الأجهزة الالكترونية في انه يحتوي على مصدر حراري متغير الفيض الحراري. تم إجراء تحويل المعادلات الواصفة للسريان و انتقال الحرارة الطبيعي إلى صورة لا بعدية مناسبة وأدى ذلك إلى الحصول على معادلات لابعدية تشتمل على العوامل التي لها تأثير على التوزيع الحراري و السريان. تم حل المعادلات عددياً باستخدام طريقة الفروق المحدودة، وتم عمل برنامج للحاسب الآلي لتنفيذ هذا النموذج الرياضي المقترح في هذه الدراسة. أمكن الحصول على التوزيع الحراري وكذلك خطوط السريان خلال الحيز وكذلك رقم نوسلت. تمت دراسة عدة حالات لنوع المصدر الحراري المركز، هذه الحالات هي: مصدر حراري مركز في خط في منتصف القاعدة، وفي خطين، ثم في ثلاث خطوط موزعين بالتساوي على مساحة القاعدة، و مصدر حراري مركز وموزع توزيع متزايد على مساحة القاعدة. في هذا البحث تم اقتراح صيغة ترابطية لحساب رقم نوسلت المتوسط وذلك كدالة في كل من رقم رايلى والقطر المكافئ للفتحات

### Abstract

The study of natural convection from a heat source located at the bottom of partially top vented enclosure is presented. Air cooling for electronic component situated at the bottom of a top vented enclosure is studied theoretically. The flow is assumed to be laminar, steady and of constant physical properties. The process is described by continuity, momentum and energy partial differential equations, which are expressed in Cartesian coordinates system. Due to the nature of the studied problem and with proper transformation of the problem dependent and independent variables, these governing equations are transformed to a set of dimensionless partial differential equations. This set of differential equations is transformed to set of difference equations by the implantation of finite difference technique. Accordingly, one can obtain the solutions for this problem, which are obtained by application of the well-known Gauss Siedel iteration method. A computer program is developed to solve the present proposed mathematical model. According to this solution; the values of Nusselt number, for different values of Rayleigh number are obtained.

Comparisons between the present obtained results and those results obtained in previous theoretical results are performed for parametric variations of the vent opening size and shape. Also a correlation for Nusselt number as a function of Rayleigh number and equivalent diameter of the vent is proposed.

**Keyword:** Natural Convection- Theoretical study- Three dimensions -top- vented enclosure

### NOMENCLATURE

$A$  : Area  $m^2$

$As$  : Aspect ratio  $L_3/L_1$ , --

$C_p$  : Specific heat at constant pressure of fluid,  $J. kg^{-1}. K^{-1}$

$d$  : equivalent diameter of open, m

$h$  : Local convective heat transfer coefficient,  $W.m^{-2}. K^{-1}$

$H$  : variable Heat source,  $W. m^3$

$k$  : Thermal conductivity of the fluid,  $W.m^{-1}. K^{-1}$

$L$  : Length, m

$Nu$  : Nusselt number  $(h.L_1/k)$ , \_

$p$  : Pressure, Pa

$P$  : Dimensionless pressure, --

$Pr$  : Prandtl number, \_

$Q$  : Heat transfer rate, W

$q''$  : Heat flux,  $W.m^{-2}$

$T$  : Temperature, K

$u,v,w$  : Velocity components in  $x, y$  and  $z$  coordinates,  $m.s^{-1}$

$U,V,W$ : Dimensionless velocity components, \_

$x,y,z$  : Cartesian coordinates, m

$X, Y,Z$ : Dimensionless Cartesian coordinates  $(x/L_1, y/L_1, z/L_1)$ , \_

VAR: vent aspect ratio,  $d/L_1$ , \_

### Greek symbols

$\alpha$  : Thermal diffusivity  $(k/\rho C_p)$ ,  $m^2.s^{-1}$

$\mu$  : Dynamic viscosity,  $kg.m^{-1}.s^{-1}$

$\nu$  : Kinematic viscosity,  $m^2.s^{-1}$

$\rho$  : Density,  $kg.m^{-3}$

$\theta$ : Dimensionless temperature  $(\frac{8k}{HL_1^2}(T - T_0))$

### Subscripts

1 : length in X - direction

2 : length in Y - direction

3 : length in Z - direction

w23: Y- and Z-direction

w13: X- and Z-direction

max: maximum

### 1-Introduction

Natural convection in enclosures has attractive considerable interest of many investigators since it is very common in several engineering and environmental problems. Applications of such analysis are ranging from building design (i.e. ventilation), solar energy systems, and electronic equipment cooling, to solar collectors. Therefore a cooling by natural convection represents in several fields, where the heat to be dissipated is low enough, an attractive system in thermal control because of its low cost, reliability and simplicity in use.

Air cooling of electronic components by natural convection is important of thermal control scheme especially for compact power supplies, portable computers, and many other small electronic systems. Most of available relevant studies to such applications have

been focused on complete enclosures on the bottom of a horizontal enclosure. As an example Sezai and Mohamad [1], 2000 studied numerically natural convection in air due to a discrete flush-mounted rectangular heat source with vertically oriented discrete heating. They presented the numerical results of two-dimensional double-diffusive natural convection in a square porous cavity partially heated from below while its upper surface is cooled at a constant temperature. Aydin and Yang [2], 2002 treated numerically the convection of air in a rectangular enclosure that was locally heated from below and symmetrically cooled from the two vertical sides.

Early work on completely enclosed configurations with horizontal heating was reported by Myrum [3], 1990 studied the natural convection heat transfer from a heat source mounted flush to bottom bounding surface of an open top cylindrical cavity. Water was the transport medium. The experiments showed that the average Nusselt number based on the temperatures of the heat source and the cylinder walls was virtually unaffected by the height and the opening size of the cavity, for the range of enclosure heights, opening sizes and Rayleigh numbers considered. Several modes of flow were observed. M. Yang and W. Q. Tao [4], 1995 numerically studied the natural convection in a cubic enclosure with an internal isolated heated vertical plate. The internal plate was suspended under the lower surface of the enclosure top wall and electrically heated. The six enclosure walls were at a lower constant temperature. The range of Rayleigh number is from  $8 \times 10^4$  to  $5 \times 10^7$ . S. B. Satha and Y. Joshi [5], 1992 studied numerically combined the conduction and natural convection transport from a substrate-mounted heat generating protrusion in a liquid-filled square enclosure. The governing steady two dimensional equations were solved using finite-difference method for wide range of Rayleigh numbers, protrusion thermal conductivities and widths, substrate heights, and enclosure boundary conditions. Higher Rayleigh numbers, protrusion thermal conductivities, and widths

enhanced cooling. S. K. W. Tou and X. F. Zhang [6], 2003 have investigated numerically a three dimensional model to study the effect of top vented shape on heat transport processes in a liquid filled rectangular enclosure of finite size. Maximum Nusselt number occurs at the heater leading edge.

In general, many investigators [7 - 9] Studied, numerically, the heat transfer inside closed enclosure. T. Fusegi et al [7], 1993 studied numerically the heat transfer in three dimension natural convection inside closed enclosure. P.K. B. Cheo, et al [8], 1983 studied the effect of inclination angle in an inclined rectangular box with the lower half heated and the upper half insulated. K. C. Karki et al [9], 1983 studied numerically the effect of heated plate position on average Nusselt number.

Numerical study of convective laminar natural convection inside enclosure was studied by J. C. Crepeau et al [10], 1997. the governing equations are solved analytically to obtain the temperature distribution and in turn Nusselt number. Yasuo Kurosaki et al [11], 1996 studied analytically the heat transfer for cooling the electronic devices. The effect of Rayleigh number in local Nusselt number and in turn in heat transfer was found. A. F. Emery et al [12], 1999 studied theoretically the effect of Rayleigh number in natural convection inside a square enclosure. Air was the transport medium. The average Nusselt number based on the temperatures of the heat source and the enclosure walls was virtually unaffected by the height. In general, top vented enclosure are used to increase the rate of heat

transfer between a fluid and a solid to produce enhanced and controlled localized cooling or heating effects on plates.

In the present study, natural convection in discretely heated small rectangular enclosures with partially opening is theoretically investigated. Both conduction in the component and substrate are included.

**2-Theoretical Model**

A mathematical model is proposed to describe the natural convection heat transfer from a hot horizontal heat source. The physical description of the problem and the coordinate system considered in this model are shown in Fig.(1). The basic dimensions of the considered geometry is a three-dimensional enclosure confined by four isothermal walls at a uniform temperature of  $T_0$ . The lower and upper walls are heated and vented wall. Accordingly the problem can be, fairly, analyzed as a three dimensional free convective problem. The enclosure contains non-uniformly distributed internal heat source. The enclosure base length and width are  $L_1, L_2$  while  $L_3$  is the enclosure height. The heat source, which maintained at non-uniformly heat flux, in x- and y-direction, is buried, horizontally, in an enclosure. In the present mathematical model, the flow is assumed to be laminar, with constant physical properties. Cartesian coordinate system (x, y, z) is used to express the flow governing equations. The governing equations consist of the continuity equation, momentum equations, and energy equation, which can be written for steady state condition as:

$$\frac{\partial u}{\partial x} + \frac{\partial v}{\partial y} + \frac{\partial w}{\partial z} = 0. \dots\dots\dots (1)$$

$$w \frac{\partial w}{\partial z} + u \frac{\partial w}{\partial x} + v \frac{\partial w}{\partial y} = - \frac{1}{\rho} \frac{\partial p}{\partial z} + \frac{\mu}{\rho} \left( \frac{\partial^2 w}{\partial x^2} + \frac{\partial^2 w}{\partial y^2} + \frac{\partial^2 w}{\partial z^2} \right) + g\beta(T - T_0) \dots\dots\dots (2)$$

$$w \frac{\partial u}{\partial z} + u \frac{\partial u}{\partial x} + v \frac{\partial u}{\partial y} = - \frac{1}{\rho} \frac{\partial p}{\partial x} + \frac{\mu}{\rho} \left( \frac{\partial^2 u}{\partial x^2} + \frac{\partial^2 u}{\partial y^2} + \frac{\partial^2 u}{\partial z^2} \right) \dots\dots\dots (3)$$

$$w \frac{\partial v}{\partial z} + u \frac{\partial v}{\partial x} + v \frac{\partial v}{\partial y} = - \frac{1}{\rho} \frac{\partial p}{\partial y} + \frac{\mu}{\rho} \left( \frac{\partial^2 v}{\partial x^2} + \frac{\partial^2 v}{\partial y^2} + \frac{\partial^2 v}{\partial z^2} \right) \dots\dots\dots (4)$$

$$\rho C_p \left( w \frac{\partial T}{\partial z} + u \frac{\partial T}{\partial x} + v \frac{\partial T}{\partial y} \right) = k \left( \frac{\partial^2 T}{\partial x^2} + \frac{\partial^2 T}{\partial y^2} + \frac{\partial^2 T}{\partial z^2} \right) + H \dots \dots \dots (5)$$

Equation (1) is the continuity equation of the three dimensional flow. The velocity components in x-, y- and z-directions are *u*, *v* and *w*. Equations (2-4) are the momentum equations in both the x-, y- and z-directions. The density and pressure are denoted by  $\rho$  and  $p$ ; respectively. While  $\beta$  is the coefficient of thermal expansion. Equation (5) is the energy equation. The temperature of the fluid is denoted by *T*, while *H* is the heat source per unit time and unit volume. The thermal conductivity, density and specific heat of the fluid are denoted by *k*,  $\rho$  and  $C_p$ ; respectively. The heat source is denoted by *H* which is defined according to the following equation T. A. Myrum [3]:

$$H = 10.2 * x + 4.1 * y + 4$$

Where *x* and *y* in meter for the square base  $L_1 = L_2$

Coefficient of thermal expansion of the fluid  $\beta$  can be defined according to the relation;

$$\beta = - \frac{1}{\rho} \left( \frac{\partial \rho}{\partial T} \right)_{P = const.}$$

Equations (1-5) must satisfy the following boundary conditions; for top vented enclosure;

$$\begin{aligned} \text{At } z = 0.0, \quad 0.0 \leq y \leq L_2, \quad 0.0 \leq x \leq L_1 : u = v = w = 0.0, \frac{\partial T}{\partial y} = -\frac{q''}{k}, p = 0.0 \\ \text{At } z = L_3, \quad 0.0 \leq y \leq \frac{L_2 - d}{2}, \quad 0.0 \leq x \leq \frac{L_1 - d}{2} : u = v = w = 0.0, T = T_w, \frac{\partial p}{\partial z} = 0.0 \\ \quad \quad \quad \frac{L_2 + d}{2} \leq y \leq L_2, \quad \frac{L_1 + d}{2} \leq x \leq L_1 : u = v = w = 0.0, T = T_w, \frac{\partial p}{\partial z} = 0.0 \\ \quad \quad \quad \frac{L_2 - d}{2} \leq y \leq \frac{L_2 + d}{2}, \quad \frac{L_1 - d}{2} \leq x \leq \frac{L_1 + d}{2} : \frac{\partial u}{\partial y} = \frac{\partial v}{\partial y} = w = 0.0, \frac{\partial T}{\partial y} = 0.0, \frac{\partial p}{\partial z} = 0.0 \dots \dots (6) \\ \text{At } x = 0, \quad 0.0 \leq y \leq L_2, \quad 0.0 \leq z \leq L_3 : u = v = w = 0.0, T = T_{w23} \\ \text{At } x = L_1, \quad 0.0 \leq y \leq L_2, \quad 0.0 \leq z \leq L_3 : u = v = w = 0.0, T = T_{w23} \\ \text{At } y = 0, \quad 0.0 \leq x \leq L_1, \quad 0.0 \leq z \leq L_3 : u = v = w = 0.0, T = T_{w13} \\ \text{At } y = L_2, \quad 0.0 \leq x \leq L_1, \quad 0.0 \leq z \leq L_3 : u = v = w = 0.0, T = T_{w13} \end{aligned}$$

When *d* equals to zero is the case of closed enclosure. Solving the governing equations (1-5) with the aid of boundary conditions (6), one can obtain the temperature and velocity distribution throughout the flow field. Moreover the local Nusselt number can be estimated according to the following equation:

Where *h* is the heat transfer coefficient, which is defined according to the relation;

$$h = \frac{q''}{(T_{max} - T_0)}$$

Where  $q''$  is the heat flux. The maximum temperature of the fluid is  $T_{max}$ , while  $T_0$  is the temperature of the enclosure walls.

$$Nu = \frac{h.L_1}{k}$$

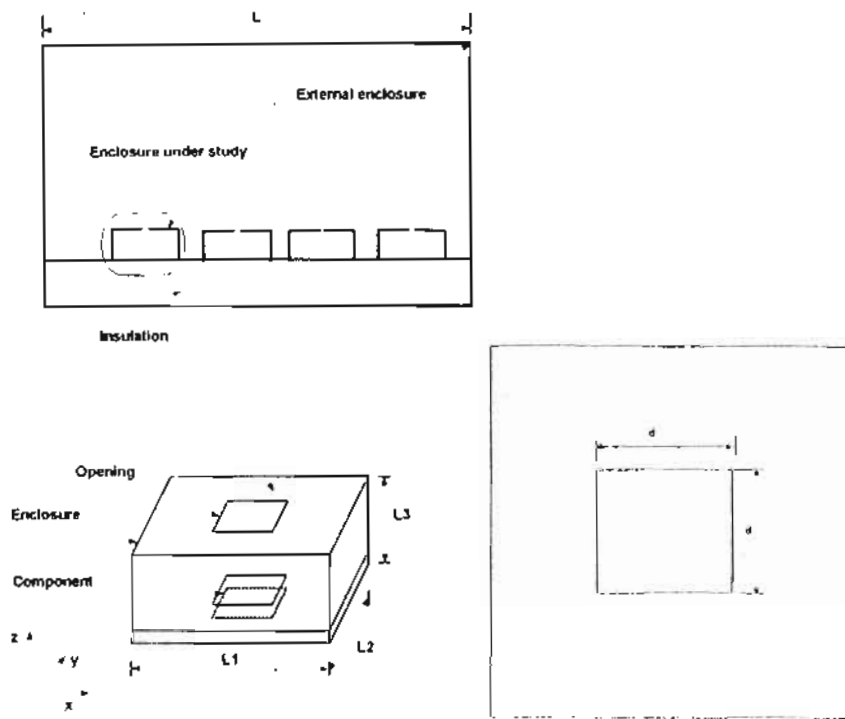


Fig.(1) Schematic diagram of the examined enclosure and the shape of vent

**2.1 Dimensionless form of the Governing equations**

In order to put the governing equations and their boundary conditions in a dimensionless form, one introduces the following dimensionless independent and dependent variables as;

$$X = \frac{x}{L_1}, Y = \frac{y}{L_1}, Z = \frac{z}{L_1}, U = u \frac{L_1}{\nu},$$

$$V = v \frac{L_1}{\nu}, W = w \frac{L_1}{\nu}, P = \frac{p}{\rho} \times \left( \frac{L_1}{\nu} \right)^2, \dots (7)$$

$$\theta = \frac{8k}{HL_1^2}(T - T_0)$$

$$\frac{\partial U}{\partial X} + \frac{\partial V}{\partial Y} + \frac{\partial W}{\partial Z} = 0 \dots\dots\dots (8)$$

$$U \frac{\partial U}{\partial X} + V \frac{\partial U}{\partial Y} + W \frac{\partial U}{\partial Z} - \nabla^2 U = - \frac{\partial P}{\partial X} \dots\dots\dots (9)$$

$$U \frac{\partial V}{\partial X} + V \frac{\partial V}{\partial Y} + W \frac{\partial V}{\partial Z} - \nabla^2 V = - \frac{\partial P}{\partial Y} \dots\dots\dots (10)$$

Where  $L_f$  is the characteristic length. It is equal to the square side length in case of a square enclosure and equals to the base length in case of a rectangular enclosure. The dimensionless  $x$ - , $y$ - and  $z$ - coordinate are,  $X$ ,  $Y$  and  $Z$ ; respectively; while  $U$ ,  $V$  and  $W$  are the dimensionless velocity component in  $X$ -,  $Y$ -and  $Z$ -direction. The kinematics viscosity is  $\nu$  and  $\theta$  is the dimensionless temperature.

Substitution with the foregoing defined dimensionless variables in equations (1-5), yields to the dimensionless form of the governing equations as;

$$U \frac{\partial W}{\partial X} + V \frac{\partial W}{\partial Y} + W \frac{\partial W}{\partial Z} - \nabla^2 W = - \frac{\partial P}{\partial Z} + 8 \frac{Ra}{Pr} \theta \dots\dots\dots (11)$$

$$U \frac{\partial \theta}{\partial X} + V \frac{\partial \theta}{\partial Y} + W \frac{\partial \theta}{\partial Z} - \frac{1}{Pr} \nabla^2 \theta = \frac{8}{Pr} \dots\dots\dots (12)$$

Where  $\nabla^2$  is the Laplacian operator,  $\left( \frac{\partial^2}{\partial X^2} + \frac{\partial^2}{\partial Y^2} + \frac{\partial^2}{\partial Z^2} \right)$ , while  $Pr$  and  $Ra$  are Prandtl and Rayleigh numbers respectively, which are defined according to the following equations;

$$Pr = \frac{\nu}{\alpha} \quad , \quad Ra = \frac{g \cdot \beta \left( \frac{L_1}{2} \right)^3 H L_1^2}{8k} \dots\dots\dots (13)$$

The dimensionless form of governing equations (8-12) must satisfy the following boundary conditions;

$$\begin{aligned} \text{At } Z = 0.0, \quad 0.0 \leq Y \leq \frac{L_2}{L_1}, \quad 0.0 \leq X \leq 1 : U = V = W = 0.0, \frac{\partial \theta}{\partial Y} = 1, P = 0.0 \\ \text{At } Z = \frac{L_3}{L_1}, \quad 0.0 \leq Y \leq \frac{L_2 - d}{2 \cdot L_1}, \quad 0.0 \leq X \leq \frac{L_1 - d}{2 L_1} : U = V = W = 0.0, \theta = 0.0, \frac{\partial P}{\partial Z} = 0.0 \\ \quad \frac{L_2 + d}{2 \cdot L_1} \leq Y \leq \frac{L_2}{L_1}, \quad \frac{L_1 + d}{2 L_1} \leq X \leq 1 : U = V = W = 0.0, \theta = 0.0, \frac{\partial P}{\partial Z} = 0.0 \\ \quad \frac{L_2 - d}{2 \cdot L_1} \leq Y \leq \frac{L_2 + d}{2 \cdot L_1}, \quad \frac{L_1 - d}{2 L_1} \leq X \leq \frac{L_1 + d}{2 L_1} : \frac{\partial U}{\partial Y} = \frac{\partial V}{\partial Y} = W = 0.0, \frac{\partial \theta}{\partial Y} = 0.0, \frac{\partial P}{\partial Z} = 0.0 \\ \text{At } X = 0, \quad 0.0 \leq Y \leq \frac{L_2}{L_1}, \quad 0.0 \leq Z \leq \frac{L_3}{L_1} : U = V = W = 0.0, \theta = \theta_{w23} \\ \text{At } X = 1, \quad 0.0 \leq Y \leq \frac{L_2}{L_1}, \quad 0.0 \leq Z \leq \frac{L_3}{L_1} : U = V = W = 0.0, \theta = \theta_{w23} \\ \text{At } Y = 0, \quad 0.0 \leq X \leq 1, \quad 0.0 \leq Z \leq \frac{L_3}{L_1} : U = V = W = 0.0, \theta = \theta_{w13} \\ \text{At } Y = \frac{L_2}{L_1}, \quad 0.0 \leq X \leq 1, \quad 0.0 \leq Z \leq \frac{L_3}{L_1} : U = V = W = 0.0, \theta = \theta_{w13} \end{aligned} \dots\dots\dots (14)$$

The governing equations (8-12) with their boundary conditions (13-14) are valid for both a uniformly distributed and concentrated heat source in the case of equal wall-temperature. In the case of different wall-temperature, using the same governing equations under their boundary conditions except for the left-wall dimensionless temperature is not equal to zero.

In the energy equation, the right-hand side of the equation  $\left( \frac{8}{Pr} \right)$  represents the heat source-term. This heat-source term appears at all the mesh-nodes in the case of uniformly distributed heat source. For the concentrated heat source, this heat-source parameter appears only at the nodes where the heat source is exists on it and it equals to zero at all the other nodes.

In order to solve the dimensionless form of governing equations (8-12), the

derivatives of the variables are replaced by the corresponding approximate finite divided differences. The first and second derivatives with respect to  $X, Y$  and  $Z$  are approximated by centered finite-divided-difference.

Figure (2) shows part of the mesh covering the flow field. Every node of the mesh is identified by three identifiers  $i, j$  and  $k$ . According to the mentioned

temperature and aspect ratio. Three types of heat source are studied, concentrated point heat source, line heat source and variable heat source. For every case, the flow pattern, isothermal lines are presented.

Accordingly, local and average Nusselt numbers are depicted.

### 3.1 Validity of the present model

In order to check the validity of the

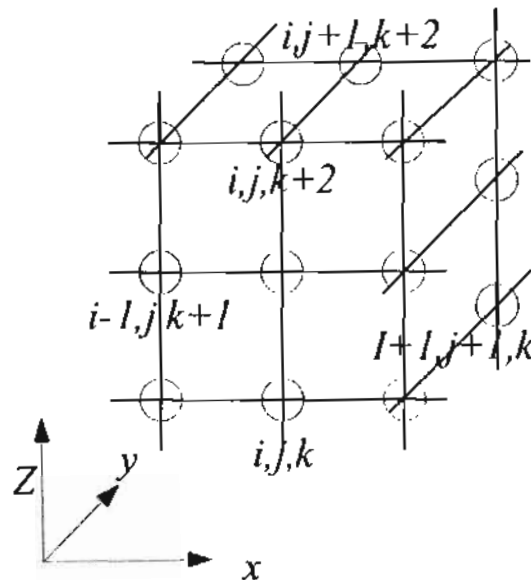


Fig. (2) Part of the used mesh

technique, momentum and energy equations are converted to four sets of algebraic equations and their boundary conditions are the final form of flow describing equations. These equations are solved, numerically, using Gauss-Seidel with relaxation iterative method. Accordingly, both hydrodynamic flow field and thermal flow field can be predicted. To determine the converged solutions correspond physically to the steady solutions. The convergence criterion for the steady state is that the change in all dependent variables between successive solution.

### 3-Results and Discussion

The proposed theoretical models are used to study the effect of Rayleigh number, dimension of open vent, wall

present proposed model, a comparison is made between the numerical results from present work with the corresponding theoretical and experimental results reported by Tou and X. F. Zhang [6], 2003

To check the validity of the present model, a comparison is made between the present results and the corresponding results after Reference [6] at the same conditions. Table (1) shows a comparison between the calculated maximum temperature after Tou and X. F. Zhang [6] and those found in the present work at Rayleigh number of  $Ra = 1 \times 10^5$ , Prandtl number of  $Pr = 0.7$  and the aspect ratio of  $As = 1$ . In this case uniformly distributed heat source is assumed. Fairly good agreement between both is found.

Also, another check of the model is made by comparing the numerical results



from present work with the corresponding experimental results reported by T. A. Myrum [3] under the same working conditions as shown in figure (3). Figure (3) illustrates the comparison between present results and result after T. A. Myrum [3]. In general the average Nusselt number takes the higher value for higher value of Rayleigh number. In the present results the average Nusselt number takes maximum values for top vented enclosure higher than for closed enclosure.

The comparisons between the present and previous study exhibit a fairly good agreement.

#### 4.2 Effect of Rayleigh number

In the following sections, the effect of the Rayleigh number on the hydrodynamic flow field and the temperature distribution is studied. One can determine the axial position from the maximum dimensionless temperature occurs.

**Table (1)** Comparison between the results of Tou and X. F. Zang [6], 2003 and the present work for a uniformly distributed heat source at  $Ra = 1 \times 10^5$  for closed enclosure

Tou and X. F. Zhang [6], 2003		Present results	
mesh size $n \times m \times m$	Max. Dimensionless temperature ( $\theta_{max.}$ )	Max. Dimensionless temperature ( $\theta_{max.}$ )	Difference %
21 × 21 × 21	0.259	0.238	8.108
41 × 41 × 41	0.264	0.247	6.44
61 × 61 × 61	0.265	0.249	6.04

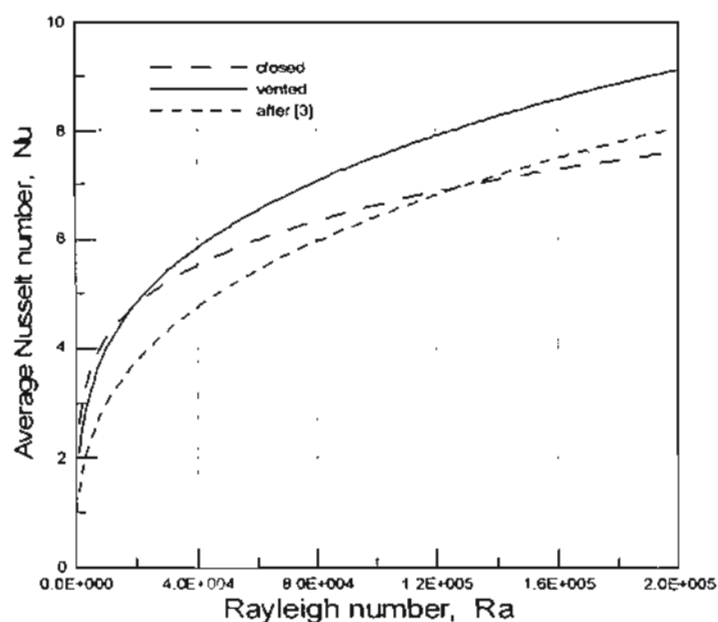


**Fig.(3)** comparison between average Nusselt number for different value of Rayleigh number

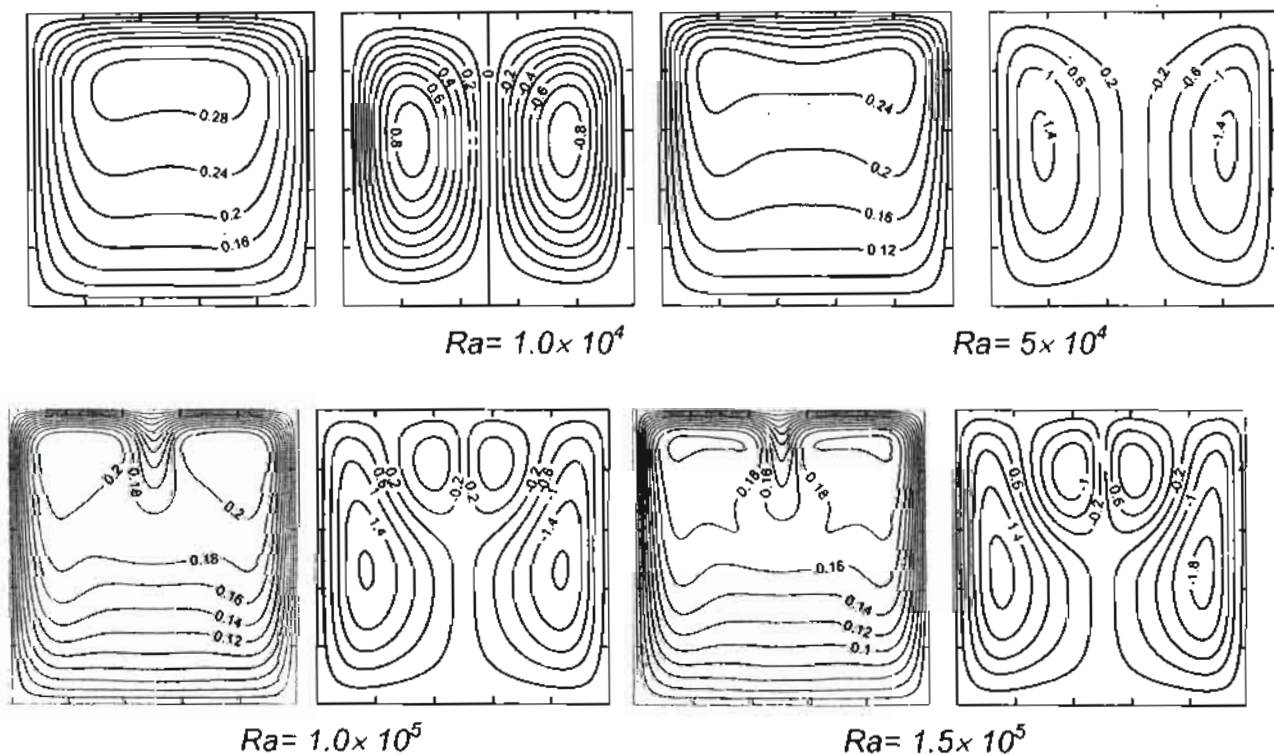
**Table (2)** Maximum dimensionless temperature and its position for different values of Rayleigh number at  $Pr = 0.70$ 

$Ra$ value	Max. Dimensionless temperature ( $\theta_{max}$ .)	Location of $\theta_{max}$
$1.0 \times 10^4$	0.289	(0.367, 0.267, 0.312) & (0.634, 0.267, 0.312)
$5.0 \times 10^4$	0.2564	(0.3, 0.267, 0.451) & (0.704, 0.267, 0.451)
$1.0 \times 10^5$	0.249	(0.267, 0.267, 0.531) & (0.734, 0.267, 0.531)
$5.0 \times 10^5$	0.226	(0.2367, 0.267, 0.582) & (0.7624, 0.267, 0.582)
$1.0 \times 10^6$	0.2038	(0.1767, 0.267, 0.652) & (0.8234, 0.267, 0.652)

Table (2) gives the value of maximum temperature and its position at different values of Rayleigh number at aspect ratio equal 1 and  $d/L_1 = 0.05$ . It is clear that, two positions inside the enclosure for the maximum temperature corresponding to every value of Rayleigh number is exist. It is noted that, with increasing Rayleigh number the value of maximum temperature ( $\theta_{max}$ ) is decreased while at low Rayleigh number the value of maximum temperature

is increased. The position of maximum temperature moves continuously toward the top wall as the Rayleigh number increases

The fluctuation of the temperature is associated with the occurrence of secondary flow as shown in Figures (4). In general, the temperature increases rapidly near the walls ( $x = 0, 1.0$ ) and more rapid decreases for higher values of Rayleigh number. In the core of the enclosure

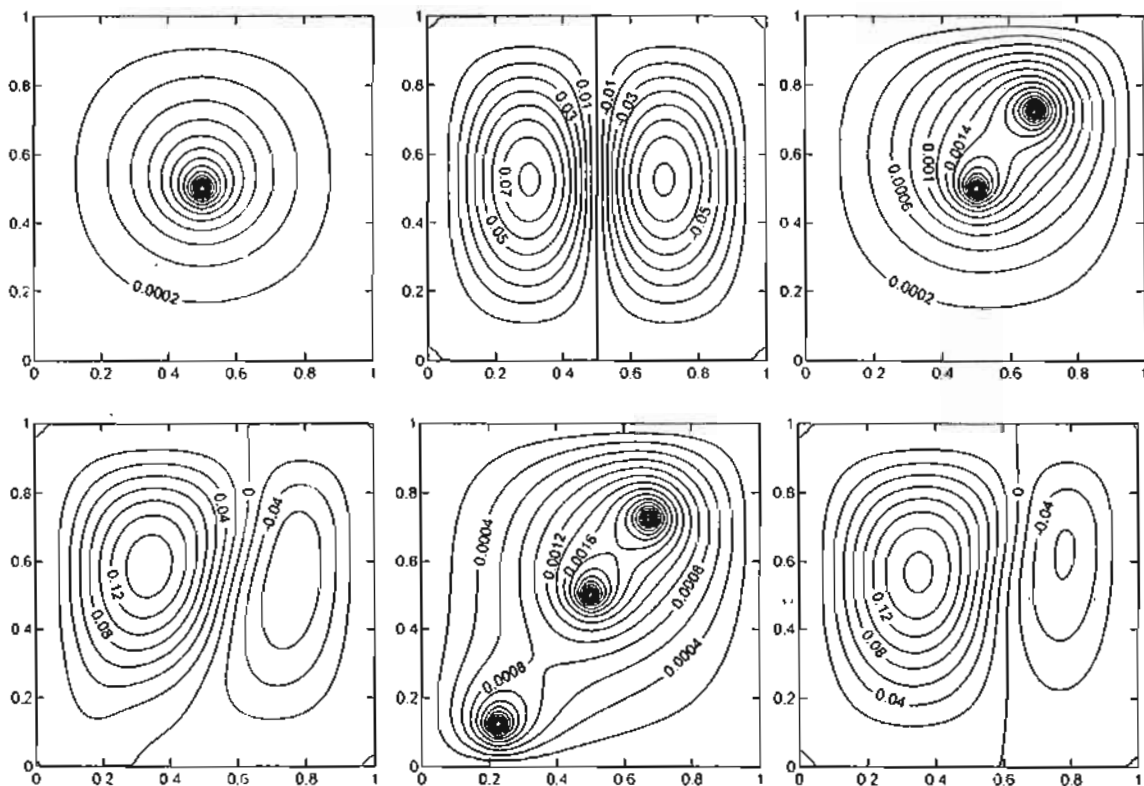
**Fig.(4)** Effect of Rayleigh number on both isotherms and streamlines at:  $Pr=0.7, Y=0.2$

(somehow far from the walls) the temperature remains almost constant, specially, for smaller values of Rayleigh number. Also, the temperature is higher as the value of Rayleigh number is smaller. The peak-value of stream function increases as Rayleigh number increases. With the values of Rayleigh number of  $1.0 \times 10^5$  and  $1.5 \times 10^5$ , variation is occurred in values of both temperature and stream function due to the existing of secondary flow adjacent to the top of the enclosure.

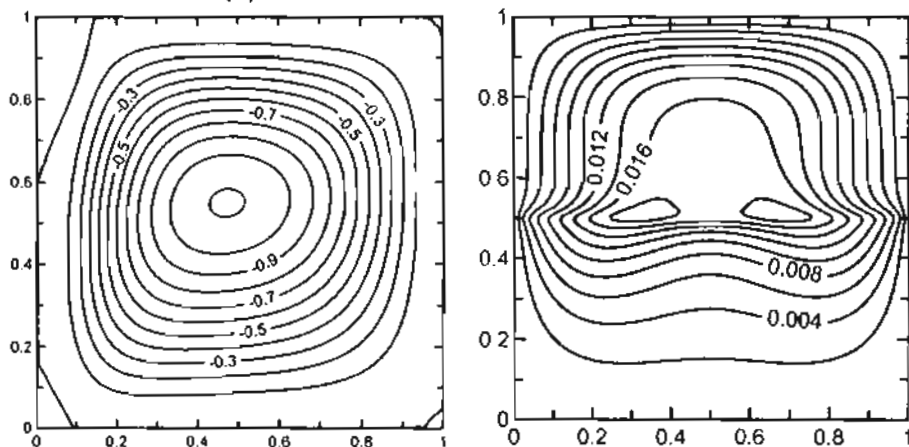
The convection flow patterns are as two

counter rotating rolls and the corresponding isotherms show a large region in which there are small regions around every point of the heat source.

Figure (5) illustrates isotherms and flow patterns in case of heat source concentrated along a horizontal line at the middle of the enclosure, at  $Y=0.5, Z=0.1$ . The convection flow pattern in the enclosure is as two symmetrical counter rotating-rolls. There are two high temperature regions in both left and right sides; and adjacent to the heat source position. The major of the heat is



(a) Isotherms and stream lines for a concentrated heat source



(b) Isotherms and stream distributed heat source along a plane parallel to the base  
 Fig.(5) Isotherms and stream distributed heat source at  $Z=0.1$  and at:  $Ra = 1.0 \times 10^5$ ,  $Pr = 0.7$

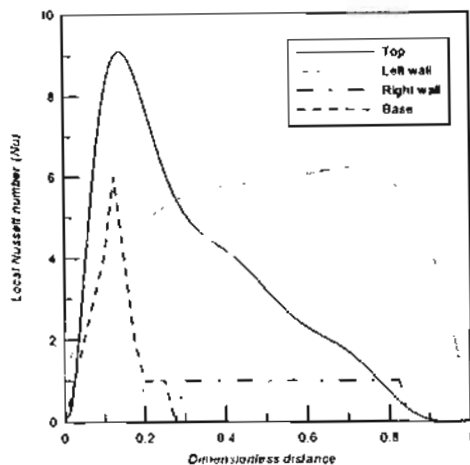


Fig.(5) Local Nusselt number for concentrated heat source along line normal to the base at  $x=0.125$

accumulated at upper of the heat source and decay rapidly near the walls. There is one high temperature region near the right end of the heat source. The distance between the high temperature region and the right side of the enclosure, decreases as the heat source for point or line increases. Near the heat source, the stream function is decayed while the temperature gradient increases rapidly. So, the conduction is predominant adjacent to location of the heat source.

Figure (5) illustrates the local Nusselt number distribution adjacent to each wall of the enclosure at  $Ra=1 \times 10^5$  for concentrated heat source along the base and lies at  $y=0.5$  and  $Z=0.0$ . The temperature increases rapidly near the walls and more rapid at the top, while no changing in temperature at the base is observed. So, the greatest value of local Nusselt number is at the top. Enclosure causes that the value of local Nusselt number at the right wall is equal it at the left wall.

### 3.3 Different wall-temperatures

The wall-temperature affects the temperature distribution and the corresponding flow patterns in the enclosure. To discuss this effect, base, right and top walls are maintained at a uniform temperature at zero dimensionless wall temperature ( $\theta=0$ ) while the left

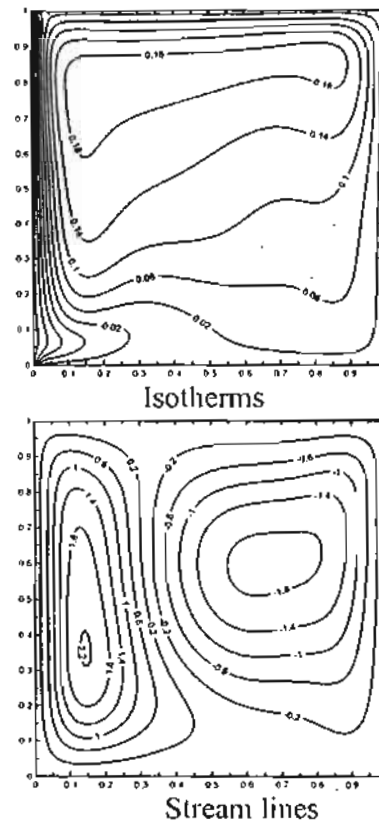


Fig.(7) Isotherms and stream lines for a uniformly distributed heat source with the left-wall temperature of  $(\theta)=-0.2$  and at:  $Ra=1.0 \times 10^5$ ,  $Pr=0.7$

wall temperature ( $\theta$ ) assigns a different value. The enclosure contains internal uniformly distributed heat source.

#### 3.3.1 Dimensionless temperature of the Left wall of -0.2

Figure (7) illustrates the temperature distribution and the corresponding flow patterns at  $Ra=1.0 \times 10^5$ ,  $Pr=0.7$  and with temperature of the left wall (Y-Z) wall equals  $(\theta=-0.2)$ . The flow patterns are as two counter-rotating rolls. The temperature gradient increases rapidly adjacent to the left and top walls. The right roll provides with a relatively higher dynamic momentum, hence it enlarges toward the left side while the left roll relatively attenuates. The high temperature region exists at vicinity of the top wall.

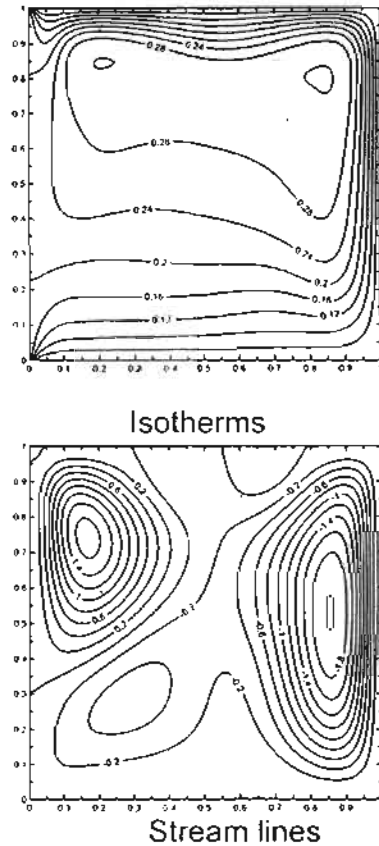


Fig.(8) Isotherms and stream lines for a uniformly distributed heat source with the left-wall temperature of  $(\theta)=0.2$  and at:  $Ra = 1.0 \times 10^5$ ,  $Pr = 0.7$

### 3.3.2 Dimensionless temperature of the Left wall of 0.2

Figure (8) illustrates the temperature distribution and the corresponding flow patterns for the same previously mentioned conditions at  $Ra = 1.0 \times 10^5$ ,  $Pr = 0.7$  except for the temperature of the left wall  $(\theta)$  is equal to 0.2. The convective flow is four-roll structure, two rolls are closed to each other and the other two rolls are separated.

The temperature gradient increases rapidly adjacent to both the right and top walls. The two-joined rolls are providing with a relatively higher dynamic momentum, hence they enlarge towards the left side while the two separated rolls attenuate and displace toward the top. Two high temperature regions exist at the vicinity of the top wall and near the two sidewalls.

The following relation correlate the results, where the local Nusselt number is

expressed as functions of Rayleigh number, Prandtl number and the equivalent diameter of the top vented

$$Nu = 0.3211 Ra^{0.364} Pr^{0.34} (1 + (d/L_t)^{0.89})$$

### 3.4 Effect of aspect ratio on Average Nusselt number

Figure (9) illustrates the average Nusselt number for different aspect ratio of top vented enclosure at  $Ra = 1.0 \times 10^5$ ,  $Pr = 0.7$ . One can show that the average Nusselt number increase for increasing aspect ratio.

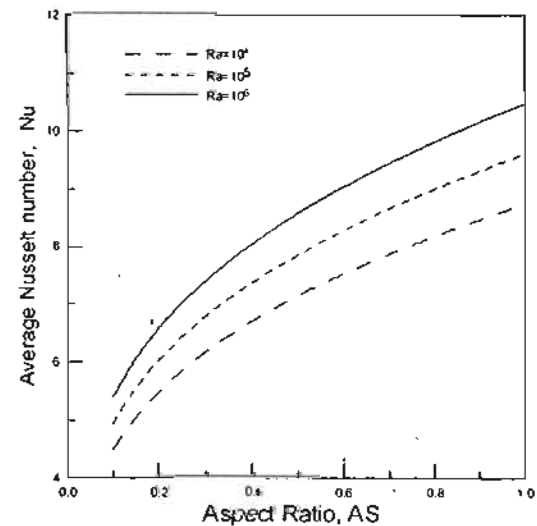


Fig.(9) Relation between average Nusselt number and Aspect ratio for different value of Rayleigh number

### 3.5 Effect of vented dimension on average Nusselt number

Figure (10) show the relation between average Nusselt number for different vent aspect ratio (VAR) of top vented enclosure at  $Ra = 1.0 \times 10^5$ ,  $Pr = 0.7$ . The average Nusselt number have a minimum value at the lowest value of vent aspect ratio and increase with increasing vent aspect ratio up to VAR=0.05, there they have a peak. Then they decrease with increasing vent aspect ratio, due to the random motion of air inside the vent and in turn, rate of heat transfer is decreased

### Conclusions

The three-dimensional natural convection in a top-vented enclosure containing a concentrated heat sources is investigated theoretically. The convective

flow is described by partial differential equations of continuity, momentum

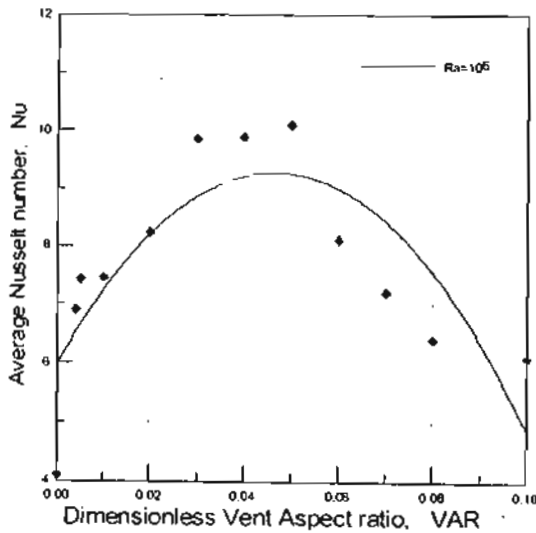


Fig.(10) Relation between average Nusselt number and vent Aspect ratio at  $Ra=10^6$ ,  $As=1.0$

and energy equations. The derivatives of the variables in the governing equations are replaced by the corresponding approximate finite differences. These equations are solved, numerically, by using gauss-seidel iterative method with relaxation. The Prandtl number ranging 0.7 to 1.0 and Rayleigh number varies from  $1 \times 10^3$  to  $1.5 \times 10^5$ . The numerical results presented in this work confirm the importance of the vent geometry in particular when the condition of compact enclosure. Comparison between the theoretical models determined in present model with previous one is good agreement.

### Reference

- [1] Sezai, A.A. Mohamad "Natural convection from a discrete heat source on the bottom of a horizontal enclosure", *Int. J. Heat Mass Transfer* 43 pp. 2257-2266, 2000.
- [2] Q.-H. Deng, G.-F. Tang, Y. Li, "A combined temperature scale for analyzing natural convection in rectangular enclosures with discrete wall heat sources", *Int. J. Heat Mass Transfer* 45, pp. 3437-3446 2002.
- [3] T. A. Myrum "Natural convection from a heat source in a top-vented enclosure" *ASME J. Heat Transfer*, Vol. 112, pp. 632-639, 1990.
- [4] M. Yang and W.Q. Tao "Three dimensional natural convection in an enclosure with an internal isolated vertical plate" *ASME J. Heat Transfer*, Vol. 117, pp.619- 625, 1995.
- [5] S. B. Sathe and J. M. Joshi "Natural convection liquid cooling of a substrate-mounted protrusion in a square enclosure: a parametric study" *ASME J. Heat Transfer*, Vol. 114, pp. 401-409, 1992.
- [6] S. K. W. Tou and X. F. Zhang "Three dimensional numerical simulation of natural convection in an inclined liquid filled enclosure with an array of discrete heaters" *Int. J. Heat Mass Transfer*, Vol. 46, No. 1, pp. 127-138, 2003.
- [7] M. W. McDonough and A. Faghri "Experimental and numerical analysis of the natural convection of water through a density maximum in a rectangular enclosure" *Int. J. Heat Mass Transfer*, Vol. 37, No. 5, pp. 783-801, 1994.
- [8] T. Fusegi, J. M. Hyun and Kunio wahara "Three dimensional natural convection in cubical enclosure with walls of finite conductance" *Int. J. Heat Mass Transfer*, Vol. 36, No. 7, pp. 1993-1997, 1993.
- [9] P. K. B. Chao, H. Ozoe, S. W. Churchill and N. Lior "Laminar natural convection in an inclined rectangular box with the lower surface half - heated and half - insulated" *ASME J. Heat Transfer*, Vol. 105, pp. 425-4328, 1983.
- [10] N. Seki, S. Fukusako and A. Yamaguchi "An experimental study of free convective heat transfer in a parallelogrammic enclosure" *ASME J. Heat Transfer*, Vol. 105, pp. 433-439, 1983.
- [11] C. J. Ho and F. J. Tu "Laminar mixed convection of cold water in vertical annulus with a heated rotating inner cylinder" *ASME J. Heat Transfer*, Vol. 114, pp. 418-424, 1992.
- [12] K. C. Karki, P. S. Sathiyammrthy and S. V. Patanker "Natural convection in partitioned cubic enclosure" *ASME J. Heat Transfer*, Vol. 105, pp. 433-439, 1983.
- [13] R. J. A. Janssen and R. A. W. M. Henkes "The first instability mechanism in differentially heated cavities with conducting horizontal wall" *ASME J. Heat Transfer*, Vol. 117, pp. 626-633, 1995.
- [14] J. C. Crepeau and R. Clarkscan "Similarity solution of natural convection with internal heat generation" *ASME J. Heat Transfer*, Vol. 119, pp.183- 185, 1997.
- [15] Arel Weisberg, Haim H. Bau and J. N. Zemel "Analysis of micro-channels for integrat cooling" *Int. J. Heat Mass Transfer*, Vol. 35, No. 10, pp. 2465-2474, 1992.
- [16] Kazuyyoshi Fushinobu, Kunio Hijikata and Yasuo Kurosaki "Heat transfer regime map for electronic devices cooling" *Int. J. Heat Mass Transfer*, Vol. 39, No.15, pp. 3139-3145, 1996.
- [17] A. F. Emery and J. W. Lee "The effect of property variations on natural convection in square enclosure" *ASME J. Heat Transfer*, Vol. 121, pp.57-62, 1999.